Synthesis and Excited State Dynamics of μ-Oxo Group IV Metal Phthalocyanine Dimers: A Laser Photoexcitation Study

Anna Paola Pelliccioli,[†,‡] Kevin Henbest,[†,§] Gwanghoon Kwag,[||] Terri R. Carvagno,[||] Malcolm E. Kenney,*[,||] and Michael A. J. Rodgers*[,†,⊥]

Center for Photochemical Sciences and Department of Chemistry, Bowling Green State University, Bowling Green, Ohio 43403, and Department of Chemistry, Case Western Reserve University, Cleveland, Ohio 44106

Received: October 2, 2000; In Final Form: January 4, 2001

The synthesis of two metal phthalocyanine monomers, GePc[OSi(n-$C_6H_{13})_3]_2$ and SnPc[OSi(n-$C_6H_{13})_3]_2$, and two μ-oxo-bridged dimers, (n-$C_6H_{13})_3$SiOSiPcOGePcOSi(n-$C_6H_{13})_3$ and (n-$C_6H_{13})_3$SiOSiPcOSnPcOH, are described. The ground-state absorption spectra and excited-state dynamics of these compounds together with those of (n-$C_6H_{13})_3$SiOSiPcOSiPcOSi(n-$C_6H_{13})_3$ have been measured. The absorption spectra of the dimers are blue shifted with respect to the monomers and whereas the latter exhibit a strong fluorescence in the visible, the dimers show only a weak emission in the near-IR. These observations are characteristic for the presence of exciton interactions in all three dimers, as had been reported earlier for the Si−O−Si dimer. Subnanosecond laser flash photolysis experiments on all five compounds yielded triplet−triplet absorption spectra, triplet lifetimes, triplet quantum yields, and bimolecular rate constants for quenching of the triplet states by O_2. The triplet quantum yields and lifetime for the monomers and the dimers were fairly similar. The oxygen quenching rate constants indicate a diffusion-controlled energy transfer process for the monomers, but in the case of the dimers, these rate constants are up to 2 orders of magnitude less. Singlet oxygen quantum yields were measured. These are close to the triplet yields for the monomers, but markedly less for the dimers. These results were interpreted as resulting from reversible energy transfer in the dimers in competition with quenching to the ground-state surface. Reversible energy transfer with molecular oxygen occurs because the dimer triplet energies are significantly lower than those of the monomers, probably because of charge resonance interactions between the closely lying π-planes. The reversible energy transfer kinetics allow estimation of the triplet energies which are 1−2 kcal mol^{-1} lower than the energy gap in oxygen (22.5 kcal mol^{-1}). Ultrafast pump−probe spectrometry measurements were used to investigate the early dynamic events in the dimers. It has been determined that the rate constant for intersystem crossing between the dimer lower exciton state and the triplet state was near 10^{-10} s, varying somewhat with central metal. Experiments at high time resolution indicated that the lower exciton state is formed initially in a torsionally excited state, the cooling of which has a lifetime of about 10 ps.

Introduction

Silicon, germanium, and tin form oxygen-bridged stacks containing two or more macrocycles where the stack axis is formed by a linear chain of M−O-M−O− bonds and the phthalocyanine π-planes are disposed approximately perpendicular to the stacking axis. Such compounds have captured the interest of synthetic chemists, spectroscopists, and theoreticians since first discovered 4 decades ago.[1−15] The simplest members of these oligomers are the μ-oxo dimers (Figure 1 shows Si−O−Si variant) which have been prepared and characterized by spectroscopic, structural, and theoretical investigations.[5,6,8,9,11−15] An easily observable difference between the μ-oxo dimers and the corresponding monomers is in the UV−vis absorption spectra of solutions in solvents such as toluene, where the dimer spectra show significant blue shifts in the long wavelength absorption bands. This is understood as arising from a splitting of the normally degenerate orbitals of the separated monomers under the influence of the interaction between the two cofacially aligned π-orbitals.[6,16,17] Thus, the first excited singlet state of the dimer is composed of a pair of exciton states that are different in energy by an amount that depends, inter alia, on the inter-plane spacing. Optical transitions originating from the ground state (S_0) are allowed only to the upper exciton state, $|+\rangle$, hence the spectral blue shift. Population of the upper state by light absorption is followed by internal conversion to the lower exciton state, $|-\rangle$, from which radiative processes are forbidden. The question is thus raised as to how the proximity of interacting π-systems in the dimers affects the excited-state dynamics and the nature of the intermediate states. Oddos-Marcel et al. addressed this question and reported that an Si−O−Si dimer shows a very weak, very red-shifted fluorescence which they attributed to transitions from $|-\rangle$, to a higher vibrational level of the ground state.[14] They estimated a singlet state lifetime of 24 ps. Furthermore, Ferencz et al.[13] addressed the same question for the two rings in a tetra-(methoxy)-tetra-(octyloxy)-substituted silicon phthalocyanine dimer. They reported a pronounced solvato-chromism of the ground-state

* To whom correspondence should be addressed.
† Center for Photochemical Sciences and Department of Chemistry.
‡ Current address: Institute of Physical Chemistry, University of Basel, CH.
§ Current address: Department of Chemistry, Clemson University, Clemson, SC 29634.
|| Department of Chemistry.
⊥ E-mail: rodgers@bgnet.bgsu.edu. Fax: 419-372-9300.

10.1021/jp003599y CCC: $20.00
Published on Web 02/20/2001

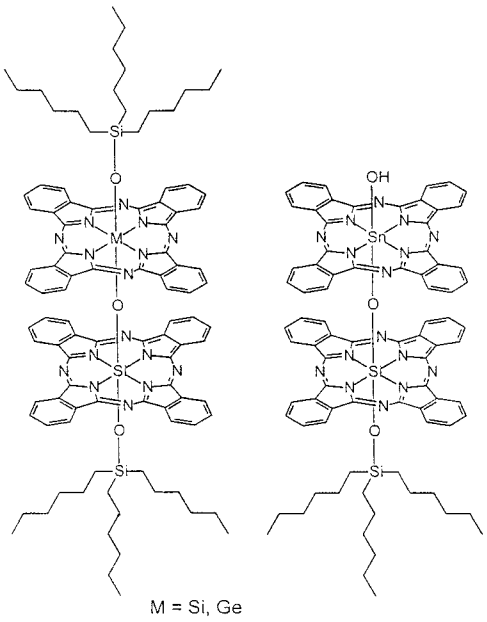

Figure 1. Structures of $(n\text{-}C_6H_{13})_3SiOSiPcOSiPcOSi(n\text{-}C_6H_{13})_3$, $(n\text{-}C_6H_{13})_3SiOSiPcOGePcOSi(n\text{-}C_6H_{13})_3$. and $(n\text{-}C_6H_{13})_3SiOSiPcOSnPcOH$.

absorption and characterized a triplet state via nanosecond laser flash photolysis studies (vide infra). That photoexcitation leads to excitonic behavior in the stacks has prompted researchers to propose that such systems might have a role in the development of photoactive devices.[18,19] Recently Ern et al. have employed ultrafast pump−probe spectrometry to study exciton migration in (phthalocyanato)polysiloxane.[20]

The present contribution contains descriptions of the synthesis and a spectrometric study of the excited-state dynamics of dimers having Si−O−Ge and Si−O−Sn backbones, i.e., $(n\text{-}C_6H_{13})_3SiOSiPcOGePcOSi(n\text{-}C_6H_{13})_3$ and $(n\text{-}C_6H_{13})_3SiOSiPcOSnPcOH$, and the excited-state dynamics of a dimer having an Si−O−Si backbone, i.e., $(n\text{-}C_6H_{13})_3SiOSiPcOSiPcOSi(n\text{-}C_6H_{13})_3$. Triplet state quantum yields, triplet energies, and oxygen quenching rate constants for these dimers are reported, as are intersystem crossing rate parameters and some information on very early dynamic events.

Experimental Section

Syntheses. *SiPc[OSi(n-C₆H₁₃)₃]₂*. A preparation of this compound has been described.[21]

GePc[OSi(n-C₆H₁₃)₃]₂. A mixture of $GePc(OH_2$22 (45.7 g, 0.0739 mol), $(n\text{-}C_6H_{13})_3SiOH$[23] (80 mL, 0.21 mol) and toluene (4.0 L) was slowly distilled in an apparatus equipped with a Dean−Stark trap for 3 h (362 mL of distillate), and then filtered. The solid was washed (toluene), and the filtrate and washings were combined, concentrated to an oil by rotary evaporation (70 °C), diluted with CH_3OH (50 mL), and filtered. The solid was washed (CH_3OH), vacuum-dried (66 °C) and weighed (42.7 g, 49%). Part of this product (99.0 mg) was chromatographed (Al_2O_3V, 1:1 hexanes:toluene solution), washed (CH_3OH), vacuum-dried (66 °C), and weighed (65.7 mg, 66%). NMR (300 MHz, C_6D_6): δ 9.72 (m, 1,4-Pc H), 7.90 (m, 2,3-Pc H), 0.92 (m, ϵ-CH_2), 0.80 (t, CH_3), 0.54 (m, δ-CH_2), 0.25 (m, γ-CH_2), −0.85 (m, β-CH_2), −2.00 (m, α-CH_2). Anal. Calcd for $C_{68}H_{94}GeN_8O_2Si_2$: C, 68.96; H, 8.00; Ge, 6.13. Found: C, 68.75, H, 7.49, Ge, 6.52. HRMS−FAB (*m*/*z*): $[M]^+$ calculated for $C_{68}H_{94}70GeN_8O_2Si_2$, 1180.6281; found 1180.6285, 1180.6270.

The compound is a turquoise solid. It is soluble in pentanes, toluene, and CH_2Cl_2. In later work, it was found that the yield of the compound could be improved by purging the toluene with N_2, conducting the synthesis under N_2 and extending the reaction time to 5 h.

SnPc[OSi(n-C₆H₁₃)₃]₂. Under N_2, a mixture of $SnPc(OH)_2$-24 (830 mg, 1.32 mmol), $(n\text{-}C_6H_{13})_3SiOH$ (1.2 g, 4.0 mmol) and toluene (80 mL) was slowly distilled in an apparatus equipped with a Dean−Stark trap for 2 h (∼20 mL of distillate), and then filtered. The solid was washed (toluene), and the filtrate and washings were combined and evaporated to dryness by rotary evaporation (∼40 °C). The residue was washed (pentane), vacuum-dried (∼60 °C), and weighed (570 mg, 35%). NMR (300 MHz, C_6D_6): δ 9.66 (m, 1,4-Pc H), 7.86 (m, 2,3-Pc H), 0.95 (m, ϵ-CH_2), 0.80 (t, CH_3), 0.56 (m, δ-CH_2), 0.26 (m, γ-CH_2), −0.75 (m, β-CH_2), −1.84 (m, α-CH_2).

The compound is a blue solid. It is soluble in hexanes, toluene, and CH_2Cl_2.

(n-C₆H₁₃)₃SiO₂SiPcOSiPcOSi(n-C₆H₁₃)₃. A preparation of this compound has been given previously.[21]

(n-C₆H₁₃)₃SiOSiPcOGePcOSi(n-C₆H₁₃)₃. A mixture of $(n\text{-}C_6H_{13})_3SiOSiPcOGePcOH$[25] (273) mg, 0.188 mmol), $(n\text{-}C_6H_{13})_3SiOH$ (220 mg, 0.732 mmol), and toluene (15 mL) was slowly distilled for 1 h (∼5 mL of distillate), filtered, and then evaporated to a semisolid by rotary evaporation (∼70 °C). The semisolid was extracted with CH_3OH (10 mL), washed (CH_3OH, pentane), vacuum-dried (∼ 60 °C), and weighed (225 mg, 69%). NMR (300 MHz, C_6D_6): δ 9.22 (m, 1,4-Pc H), 8.05 (m, 2,3-Pc H), 0.59 (m, ϵ-CH_2, CH_3), 0.07 (m, δ-CH_2), −0.35 (m, γ-CH_2), −1.74 (m, GePc β-CH_2), −1.84 (m, SiPc β-CH_2), −2.95 (t, GePc α-CH_2), −3.09 (t, SiPc α-CH_2). HRMS−FAB (*m*/*z*): $[M]^+$ calculated for $C_{100}H_{100}N_{16}O_374GeSi_3$, 1740.7474; found 1740.7417, 1740.7455.

The compound is a blue solid. It is soluble in hexanes, toluene, and CH_2Cl_2.

(n-C₆H₁₃)₃SiOSiPcOSnPcOH. A mixture of $SnPc(OSi(n\text{-}C_6H_{13})_3)_2$ (140 mg, 0.114 mmol), $HOSiPcOSi(n\text{-}C_6H_{13})_3$26 (94 mg, 0.11 mmol), and xylenes (70 mL) was refluxed for 4.5 h, and then evaporated to dryness by rotary evaporation (∼50 °C). The solid was stirred with a solution of dichloroacetic acid (20 μL, 0.24 mmol) and toluene (20 mL) for 2 h, and the resultant was evaporated to dryness by rotary evaporation (room temperature). The solid was stirred with a pyridine−water solution (4:1, 30 mL) at a moderate temperature (∼ 50 °C) for 5 h, and the resulting suspension was filtered. The solid was washed (1:1 toluene-hexane solution), extracted into CH_2Cl_2 (10 mL), recovered by rotary evaporation (room temperature), vacuum-dried (room temperature), and weighed (25 mg, 15%). NMR (300 MHz, $CDCl_3$): δ 9.07 (m, 1,4-SiPc H), 8.92 (m, 1,4-SnPc H), 8.42 (m, 2,3-SnPc H), 8.27 (m, 2,3-SiPc H), 0.43 (m, ϵ-CH_2, CH_3), −0.18 (m, δ-CH_2), −0.63 (m, γ-CH_2), −2.21 (m, β-CH_2), −3.40 (m, α-CH_2). HRMS−FAB (*m*/*z*): $[M - OH]^+$ calcd for $C_{82}H_{72}N_{16}O_3Si_2116Sn\ (M - OH)^+$, 1483.4505; found 1483.4462, 1483.4554.

The compound is a blue solid. It is soluble in toluene and CH_2Cl_2, but insoluble in hexanes.

Fluorescence Spectra. Fluorescence spectra up to 800 nm were monitored using a Spex Fluorolog 2, with 1 mm slits. All spectra were corrected for the sensitivity of the photomultiplier tube.

The fluorescence quantum yields were calculated using Rhodamine 101 in EtOH as a standard ($\Phi_F = 1.0$).[27] Excitation wavelengths corresponding to S_0 to S_1 and S_0 to S_2 transitions were employed. The sample and reference solutions were prepared with the same absorbance (A_i) at the excitation wavelength (near 0.06 per cm). All solutions were air saturated.

The areas under the fluorescence spectra (G_i) were measured and fluorescence quantum yields were calculated according to

$$\Phi_F^X = \frac{A_{REF} G_X n_X^2}{A_X G_{REF} \cdot n_{REF}^2} \cdot \Phi_F^{REF}$$

where the n terms are the solvent refractive indices.

Near-IR Emission Spectra. The samples were excited with the 633 nm line of a 40 mW He−Ne laser, using an optical fiber to direct the excitation beam to the cuvette. Fluorescence signals were detected with a Bruker Equinox 55 Fourier Transform spectrometer configured for near-IR emission measurements as described.[28] Spectra only were recorded. All samples were dissolved in toluene at room temperature.

Transient Absorption Spectra and Kinetics. Transient spectra were recorded in deaerated toluene (prepared by bubbling with N_2 for several minutes). The excitation beam was a 6 ns pulse of 355 nm radiation obtained from a Surelight I (Continuum) Q-switched laser. The laser energy incident at the sample was attenuated to a few mJ per pulse. Time profiles at a series of wavelengths from which point-by-point spectra were assembled were recorded with the aid of a PC controlled kinetic absorption spectrometer that has been described earlier.[29] The concentrations of the target compounds were typically 2−3 μM providing $A_{355} = 0.2$ in a 10 mm cuvette.

Triplet Quantum Yields. The relative actinometry method was used to measure the product $\Phi_T\epsilon_T$. Tetraphenylporphine (TPP) was used as reference. The solutions of sample and reference (in benzene) were arranged to have matching absorbance of ∼0.2 at 355 nm in 10 mm cuvettes. The triplet state decay profiles were recorded in air saturated solutions at 440 nm for TPP and at 500 nm for the MPc compounds (vide infra). Values of ΔA_{440} and ΔA_{500} were recorded immediately post-pulse (zero time) prior to any decays occurring. The following was employed to calculate $\Phi_T\epsilon_T$ for the unknown (X):

$$\Phi_F^X \epsilon_T^X(500) = \frac{\Delta A_{500}}{\Delta A_{440}} \Phi_T^{REF} \epsilon_T^{REF}(440)$$

The value employed for Φ_T(TPP) was 0.82.[30] The extinction coefficients at 500 nm were determined by the energy transfer method using TPP as the energy donor. With TPP for the determination of $\Phi_T\epsilon_T$ and observing at the same wavelength (440 nm) results in cancelation of the ϵ_T parameters in the calculation.

The excitation pulses were obtained from an Opotek *Magic Prism* tuned to 490 nm. This OPA was pumped by the 355 nm beam from the Surelight. The laser energy was ∼3 mJ per pulse. The absorbance of TPP at 490 nm was ∼0.1, and solutions in benzene were deaerated by bubbling with nitrogen. The rate constant for the decay of TPP triplet in the absence of added metal phthalocyanine (k_d) was determined. Phthalocyanine concentrations in the range $1-1.5 \times 10^{-5}$ M were used. This concentration was insufficient to give rise to quantitative transfer of all TPP triplets to metal phthalocyanine, but this was corrected for (vide infra). The rate of formation (k_{obs}) of the phthalocyanine triplet state absorbance was observed at 500 nm. This is an isosbestic point in the transient absorption spectrum of TPP. The decay kinetics of TPP triplet were recorded at 440 nm, which provided the value of ΔA at time zero. The value of ΔA at time zero for the phthalocyanine triplet was obtained from the fitting of the kinetics at 500 nm. To calculate the required extinction coefficients, the method of Carmichael and Hug was employed:[31]

$$\epsilon_{440}^X = \epsilon_{500}^{TPP} \cdot \frac{\Delta A_{500}}{\Delta A_{440}} \cdot \frac{k_d}{k_{obs} - k_d}$$

Singlet Oxygen Quantum Yields. Singlet oxygen quantum yields were measured using the time-resolved method employing a germanium photodiode-amplifier unit operated at 77 K (Applied detector Corporation, model 403L). The details of the method have been published.[32] Benzophenone in benzene solution was employed as reference ($\Phi_\Delta = 0.29$[33,34]). The excitation wavelength was 355 nm. Incident laser energies at the sample were near 7 mJ and a polarizing attenuator was employed to vary the excitation energy. Solutions of unknown and reference were prepared in air-saturated solution of benzene with matching absorbance of 0.5 in 10 mm cuvettes.

For the monomeric metal phthalocyanines the singlet oxygen near-IR luminescence time profiles for reference and unknown were recorded as a function of laser energy. The individual time profiles were fitted to obtain singlet oxygen lifetimes and the amplitudes of the luminescence at zero time. The latter were plotted against the laser energy and the slope (Z) of the low energy, linear portions were employed to compute the quantum yields according to the equation

$$\Phi_\Delta^{PC} = \Phi_\Delta^{REF} \cdot \frac{Z_{PC}}{Z_{REF}}$$

For the dimers, it was not possible to determine the Φ_Δ using this method because of their very low values. These values were determined by using higher laser energy and comparing the time zero singlet oxygen emission to that obtained from a benzophenone solution at the same laser energy. To correct for the fraction of donor triplet states not scavenged by oxygen at air saturation, the following expression was used:

$$\Phi_\Delta^{max} = \frac{\Phi_\Delta^{air}(k_0 + k_Q[^3O_2])}{k_Q[^3O_2]}$$

k_0 is the rate constant for the triplet state decay in the absence of oxygen, k_Q is the bimolecular rate constant for oxygen quenching, $\Phi_\Delta{}^{air}$ is the singlet oxygen quantum yield in air saturated solution, and $[^3O_2]$ is the oxygen concentration in the air-saturated benzene.

Ultrafast Pump−Probe Measurements. The pump−probe instrument for performing ultrafast (ca. 200 fs rise time) transient absorption measurements has been described.[35] Improvements have been confined to the spectrographic system for the purpose of improving signal-to-noise characteristics. To this end the double beam system outlined earlier has been replaced by a single spectrograph (Ocean Optics PC2000) and a chopper in the pump beam. Thus, the instrument is now a single beam spectrometer with alternating excitation/no excitation cycles. The computer software takes care of whether a particular signal is pump-on or pump-off. In this way every pump-on signal is referenced to a pump-off signal a few milliseconds away. This minimizes noise introduced due to instabilities in the continuum output. Noise amplitude below 1 milli-absorbance unit is commonplace with the current arrangement.

In the current experiments excitation was at 400 nm (the second harmonic of the Ti−Sapphire output), or at 640 nm, derived from an optical parametric amplifier (SpectraPhysics OPA 800).

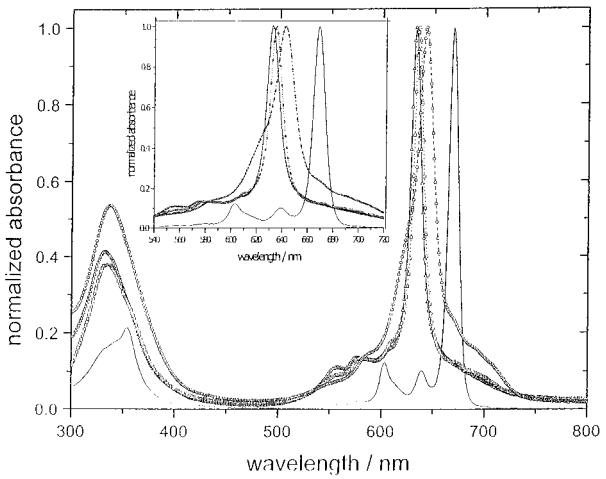

Figure 2. Normalized ground-state absorption spectra of the three μ-oxo dimers and the Si monomer for comparison. Triangles: Si−O−Sn. Squares: Si−O−Ge. Circles: Si−O−Si. Full line: monomer. The inset shows an expansion of the Q-band region.

TABLE 1

Pc	λmax/nm (ϖ/cm-1)	$\Delta\varpi$/cm^{-1} [a]	Interring spacing/pm[b]	Si−O-M distance/pm[c]
Si	668.5 (14,960)			
Ge	673.7 (14,843)			
Sn	680.0 (14,706)			
Si−O−Si	632.0 (15,823)	863	333	302
Si−O−Ge	635.1 (15,746)	786	343	316
Si−O−Sn	642.4 (15,567)	607	358	346

[a] Wavenumber differences between Si monomer and Si−O-M dimer peaks. [b] From the X-ray crystallographic data [Dirk et al.[7]] for the polymers $[SiPcO]_n$, $[GePcO]_n$, and $[SnPcO]_n$. The Si−O−Ge and Si−O−Sn values listed here were calculated as the arithmetic mean of the values for the corresponding homopolymers, reported by Dirk et al.[7] as 353 pm (Ge homopolymer) and 382 pm (Sn homopolymer). [c] Obtained by the addition of the Si−O covalent bond distance to itself (for Si−O−Si), or to that of the Ge−O and Sn−O covalent bond distances. [Emsley, J. *The Elements*; Clarendon Press: Oxford, 1989.]

Results

Ground-State Absorption Spectra. The UV−vis absorption spectra of the Si−O−Si, Si−O−Ge, and Si−O−Sn dimers were measured in toluene solutions at ca. 3 μM concentration. These spectra, normalized to unit absorbance at the respective wavelength maxima, are displayed in Figure 2. The UV−vis spectrum of the monomeric compound $SiPc(OSi(n\text{-}C_6H_{13})_3)_2$ is presented in Figure 2 for comparison. The three dimers all contain one O−SiPc component. The inset in Figure 2 shows details of the Q-band region (540 nm to 720 nm) of the spectra displayed in the main figure. The dimers all show significant blue shifts as compared to the monomer, in both Soret and Q-band regions. Table 1 lists the wavelength maxima for the three dimeric compounds and the marker compound, SiPc; in addition the spectral shifts (in terms of wavenumber) are summarized in Table 1. In addition Table 1 contains relevant data on the ring−ring spacing.

In addition to the blue shift, Figure 2 also shows that the Q-band peaks of the three dimers have intense, narrow central peaks with lower intensity wings stretching out to the red and blue sides of the central feature.

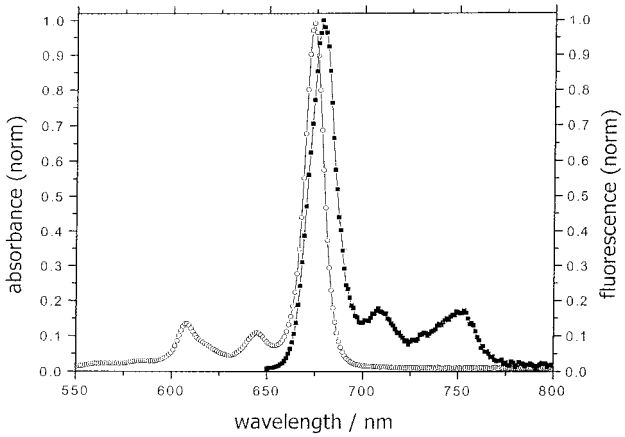

Figure 3. The ground-state absorption spectrum (open circles) and the fluorescence spectrum (full line) of the Ge monomer in toluene solution. The spectra have been normalized to unity at the respective maxima.

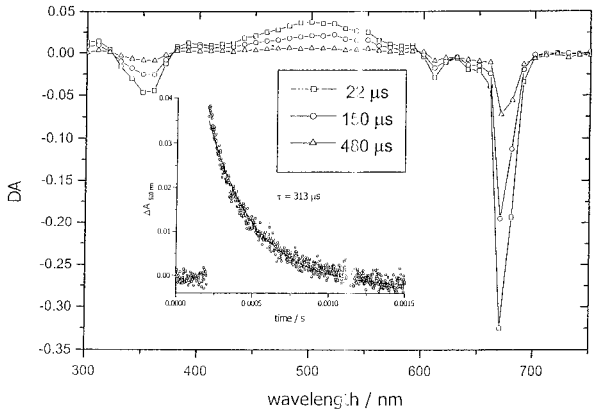

Figure 4. Transient absorption spectra recorded at three different times (as shown) after a 6 ns pulse of 355 nm light had irradiated a ca. 5 μM solution of Sn Pc monomer in toluene. The inset shows the time profile of the decay at 530 nm and a superimposed exponential fit.

Fluorescence Spectra and Quantum Yields. The Ge and Sn monomers are typical p-block metal-centered phthalocyanines and exhibit respectable fluorescence. Figure 3 shows the absorption and fluorescence spectra (normalized to unit amplitude at their respective maxima) for the Ge monomer. Quantum yield values are 0.60 for the Ge monomer in toluene and 0.18 for the Sn monomer in the same solvent, independent of the excitation wavelength. Examination of the Si−O−Ge and Si−O−Sn dimers for fluorescence showed weak signals in the near-infrared region between ca. 7000 and 12000 cm^{-1}, as reported by Oddos-Marcel et al. for a Si−O−Si dimer.[14]

Transient Spectra and Kinetics: Suprananosecond. Deaerated solutions (ca. 3 μM) of the three μ-oxo dimers and the Sn and Ge monomers in toluene were subjected to laser flash excitation (6 ns pulse duration) at 355 nm. The resulting transient absorbance time profiles were recorded point-by-point over the wavelength range 300−800 nm at 5 nm intervals with the aid of a computer-assisted kinetic absorption spectrometer. The absorbance−time-wavelength data were assembled into time-resolved spectra such as shown in Figure 4 (for the Sn monomer) and Figure 5 (for the Si−O−Sn dimer). Representative time profiles are included as insets in these figures. All compounds studied showed similar spectral features, viz., negative absorptions (bleaching) in the Soret and Q-band regions and a broad positive absorption peaking near 500 nm. Additionally in the case of the dimers a positive absorption appeared at the red side of the bleaching band. Under the prevailing conditions of

TABLE 2

Pc	$\epsilon_{500\,nm}$/M^{-1} cm^{-1}	τ/μs	$10^{-8}k_{O2}$/M^{-1} s^{-1}	10^{-9} k_{ISC}/s^{-1}	Φ_T	E_T/kcal mol^{-1}	F_D
Ge	27 500	309	18.0		0.26		0.26
Sn	27 400	129	19.0		0.40		0.33
Si−O−Si	21 600	116	0.20[a]	1.72	0.22	19.0	0.022
Si−O−Ge	32 000	136	0.78[a]	0.66	0.13	19.9	0.021
Si−O−Sn	23 300	32.5	2.03[a]	3.39	0.35	21.3	0.17

[a] From reversible kinetics analysis.

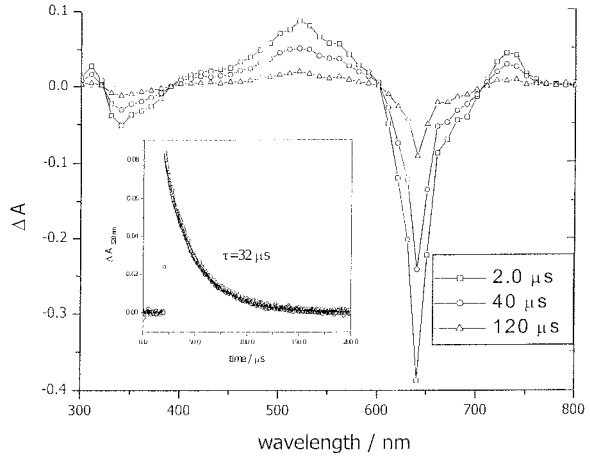

Figure 5. Transient absorption spectra recorded at three different times (as shown) after a 6 ns pulse of 355 nm light had irradiated a ca. 5 μM solution of Si−O−Sn dimer in toluene. The inset shows the time profile of the decay at 530 nm and a superimposed exponential fit.

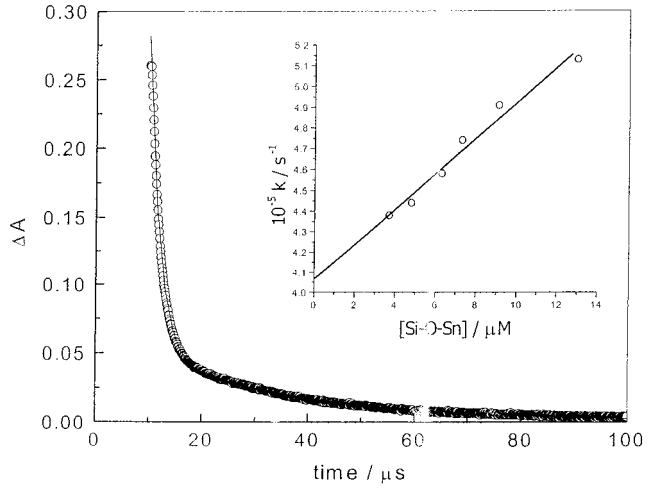

Figure 6. The main figure shows the time profile of the decay of the 530 nm transient generated by a 6 ns pulse of 355 nm light incident on a toluene solution of Si−O−Sn dimer (5μM) containing air. The circles are the data points and the full curve is a double-exponential fit. Inset: a plot of the rate constant of the first exponential contributor vs. the dimer concentration.

N_2 gas saturation the absorption features (positive and negative) recovered to the prepulse zero level according to an exponential rate law, with lifetimes above 100 μs (except for the Si−O−Sn dimer). For a given compound the bleaching recovery kinetics and the absorption decay kinetics were concomitant, and isosbestic points separated the bleaching and absorption regions. From these observations it is possible to infer that flash-induced depopulation of the ground states generates a relatively long-lived transient state, which decays to repopulate the starting material in a single-exponential process. In the succeeding Discussion section it will be argued that this state is the triplet state of the corresponding compound; in the remainder of this Results section it will be referred to as the "putative triplet state". The kinetic data for the compounds investigated are collected in Table 2.

The transient absorption kinetics are significantly changed by the addition of oxygen to the solutions of the metallophthalocyanines. In all compounds, the presence of oxygen causes both the ground-state repopulation processes and the absorption decays to recover much more quickly to the prepulse baseline levels. Within this overall picture, significant differences exist between the monomeric and the dimeric species. For the Ge and Sn monomers the 500 nm absorption (of the putative triplet state) and the 675 nm bleaching signals recovered to their respective zero levels in an exponential manner, the lifetime of which was first order in oxygen concentration. The spectrometric data lead to the bimolecular rate constants for oxygen quenching of the triplet states of the two monomers. These values are $1.78 \pm 0.05 \times 10^9$ and $1.95 \pm 0.04 \times 10^9$ M^{-1} s^{-1} for the Ge and Sn monomers, respectively, both values that are anticipated for exoergic energy transfer to oxygen from a phthalocyanine triplet state (vide infra).

The transient species (or putative triplet states) generated from excitation of the three μ-oxo dimers are also quenched by oxygen; in these cases, however, the decay profiles are sometimes exponential and sometimes not, depending on the prevailing conditions. When the exponential decay was not upheld, the time profiles were properly fitted with a sum of two exponentials. A typical example is depicted in Figure 6 (Si-O−Sn dimer) where clearly separated fast (2.1 μs) and slower (30 μs) components are seen. In the example of Figure 6 the fast component is 83% of the total signal. In a series of experiments in which the oxygen concentration was held constant (2 mM) and the dimer concentration was varied (0 through 20 μM), both the lifetime of the fast component and its fractional contribution to the total signal were found to depend linearly on the dimer concentration. An example of a plot of the rate constant of the fast component against phthalocyanine concentration is presented as an inset to Figure 6. The slope and intercept values for the three dimers were extracted (vide infra) from similar plots.

Singlet Oxygen Quantum Yields. In the anticipation that the transient absorptions near 500 nm were due to the triplet−triplet (T−T) absorptions of the compounds, it was decided to determine whether the quenching by oxygen leads to the formation of singlet oxygen-$O_2(^1\Delta_g)$. Such measurements were performed by monitoring the amplitude of the emission at 1270 nm that arises from the $^1\Delta_g \rightarrow {}^3\Sigma_g$ transition in oxygen (see Experimental Section). The emission intensity at 1270 nm from laser excitation of an unknown has been quantitatively compared with that obtained from excitation of benzophenone, under the same conditions of laser fluence and compound absorbance at the excitation wavelength. The collected data are presented in Table 2.

Extinction Coefficients and Quantum Yields. To obtain a quantitative picture of the excited-state dynamics for both the monomers and dimers, determinations were made of the intersystem crossing quantum efficiencies. This required measurements of the extinction coefficients of the triplet−triplet

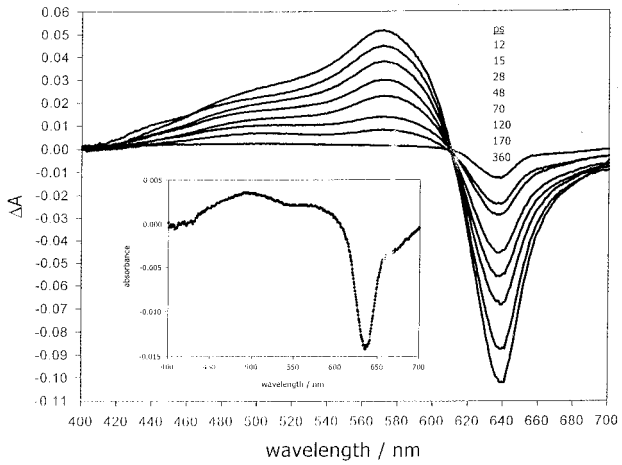

Figure 7. The main figure shows a series of absorption spectra recorded at eight time delays (as indicated) after excitation of a toluene solution of the Si−O−Sn dimer (20 μM) with a 100 fs pulse of 640 nm light. The inset shows an enlargement of the 360 ps spectrum.

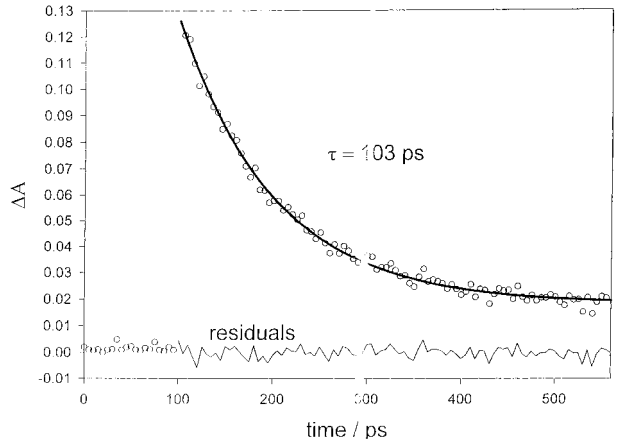

Figure 8. The time profile of the decay at 580 nm under the conditions of Figure 7. The solid curve is an exponential fit with a nonzero asymptote (see text).

absorption spectra, and those of the quantum yields for triplet formation. These experiments were performed as described in detail in the Experimental section, and the resulting data are presented in Table 2.

Transient Spectra and Kinetics: Subnanosecond. On the suprananosecond time scale, the formation of the putative triplet state absorptions (λ_{max} near 500 nm) was completed during the instrument response (ca. 10 ns). To determine the dynamics of the inter-system crossing event, ultrafast-resolved experiments were performed. For these, 100 fs pulses at 400 or 640 nm from a mode-locked, amplified, Ti-sapphire laser (with frequency doubler or OPA) were used to excite solutions of the dimers in toluene. The resulting transient absorption spectra were monitored using a pump−probe setup in which a visible coherent continuum is generated for the probe pulse. The spectra were recorded on a CCD spectrograph as described in the Experimental section. A set of transient spectra for the Si−O−Sn dimer is presented in Figure 7 which shows that a well-defined isosbestic point at 610 nm connects the positive and negative absorption signals, indicating that the 570 nm species regenerates the ground state as it decays. The inset of Figure 7 shows the spectrum recorded at a delay time of 300 ps. Comparison of this latter with the spectrum taken at a delay time of 12 ps demonstrates that significant spectral changes occur as the ground state is repopulated. The time profile of the ground-state recovery (Si−O−Sn dimer) is shown in Figure 8. The fit

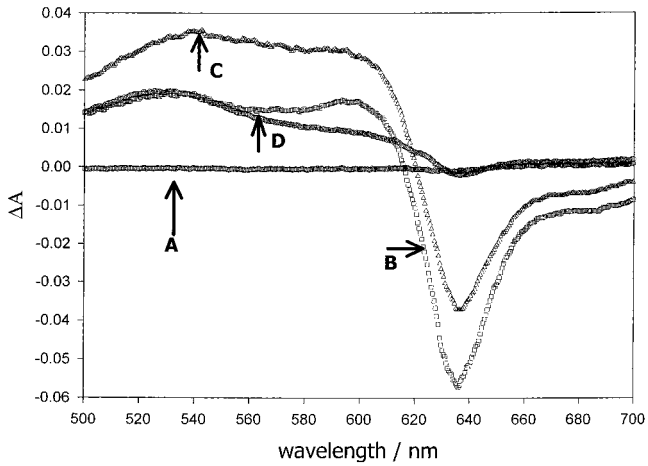

Figure 9. A series of absorption spectra recorded after excitation of a 20 μm solution (in toluene) of the Si−O−Si dimer with a 100 fs pulse at 640 nm. Delay times are as follows: A: −2.0 ps. B: 5.0 ps. C: 45 ps. D: 760 ps.

to an exponential decay with a nonzero baseline provides a lifetime of 103 ps. The other dimers show effects similar to that in Figure 8, differing only in the lifetime values. Thus, the ground-state repopulation lifetimes of the Si−O−Si and the Si−O−Ge dimers were 128 and 197 ps respectively.

The time profile in Figure 8 indicates an "instantaneous" rise of the absorption signal, however observations with higher time resolution, showed interesting details. For example, Figure 9 displays the spectral evolution in the Si−O−Si dimer over the first 45 ps after the pump pulse excitation (in addition to the spectrum at 760 ps). These show that the absorption in the 500 to 600 nm region increases during this time and that the time evolution of the spectral features depend on the detection wavelength. It is to be emphasized that there is some apparent ground-state recovery over the first 45 ps but that no isosbestic region appears between the absorption and bleaching transients. The time profiles for these changes are shown in Figure 10. Again very similar effects were observed for the other dimers.

Discussion

Syntheses. The syntheses used for the germanium and tin dimers are

$$(n\text{-}C_6H_{13})_3SiOSiPcOGePcOH \xrightarrow{(n\text{-}C_6H_{13})_3SiOH} (n\text{-}C_6H_3)_3SiOSiPcOGePcOSi(n\text{-}C_6H_{13})_3 \quad (1)$$

$$SnPc(OSi(n\text{-}C_6H_{13})_3)_2 \xrightarrow{(n\text{-}C_6H_{13})_3SiOSiPcOH} (n\text{-}C_6H_{13})_3SiOSiPcOSnPcOSi(n\text{-}C_6H_{13})_3$$

$$\xrightarrow{(1)Cl_2CHCOOH\ (2)H_2O} (n\text{-}C_6H_{13})_3SiOSiPcOSnPcOH \quad (2)$$

These two syntheses rely on known types of reactions. Attempts to prepare pure $(n\text{-}C_6H_{13})_3SiOSiPcOSnPcOSi(n\text{-}C_6H_{13})_3$ failed because of its instability to hydrolysis.

Ground-State Spectra. The UV−vis absorption spectra of the dimers and one monomer in toluene are presented in Figure 2. The absorption spectrum of the Si−O−Si dimer is identical to that published elsewhere.[5] Those of the Si−O−Ge and the Si−O−Sn dimers have not been previously published. It is generally agreed that the blue-shift arises from exciton interaction between the transition dipoles of the two planar macrocycles lying centro-symmetrically, one on top of the other without

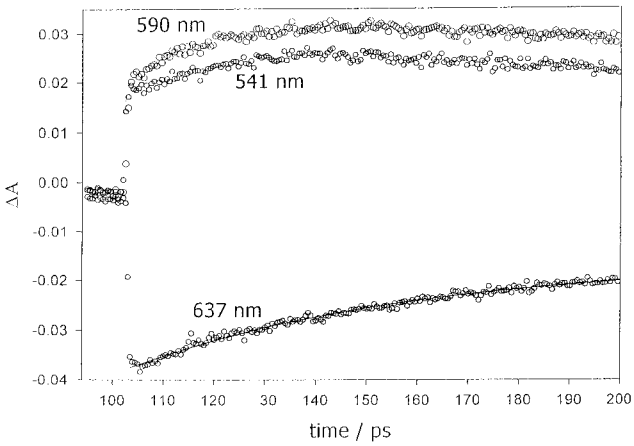

Figure 10. Time profiles taken from the experimental system of Figure 9. The wavelengths are as indicated.

molecular orbital overlap.[6] This generates a pair of new excited states, $|+\rangle$ and $|-\rangle$. In such a situation the transition from S_0 to $|+\rangle$ is allowed and that to $|-\rangle$ is forbidden.[16,17] As Figure 2 and Table 1 show, the long wavelength peak shifts to the red as M in the Si−O−M dimer changes from Si to Ge to Sn, or as the Si−O−M distance increases. Kenney and co-workers[2,22,24] prepared the three unsubstituted monomer phthalocyanines SiPc(OH)$_2$, GePc(OH)$_2$, and SnPc(OH)$_2$. Marks and co-workers[7] reported similar red shifts in the UV-vis spectra of these monomers, and they attributed these to the lower electronegativity of the larger metal atoms shifting electron density onto the π-system thereby raising the energy of the HOMO. This same shifting was found[7] to persist in homopolymers such as [MPcO]$_n$. In the hetero-dimers investigated here it is likely that the same electronegativity effects are acting, although these could be somewhat enhanced by the increasing Si−O−M distances (Table 1) causing decreasing electronic coupling between the rings as Si is replaced by Ge or Sn.

The other notable characteristics about the dimer spectra are the blue and red wings at either side of the main Q-band. Such effects have been known for Si−O−Si dimers for a number of years[5,6] and have been attributed to different torsional conformational forms of the dimers. NMR spectra have indicated that the D_{4h} symmetry species is only one of the possible torsional conformations and that, in fact, it is likely that the macrocycles can rotate freely about the Si−O−M axis.[4] Calculations by Hush and Woolsey[6] lend support to the concept that the dimers can exist in a variety of conformations about the C_4 axis.

It is assumed in the interpretation of the ground-state spectra and the other spectra of the Si−O−Sn dimer that these spectra do not significantly differ from the corresponding spectra of the analogue of the dimer having (n-C$_6$H$_{13}$)$_3$SiO groups on both ends.

Fluorescence Properties. The Ge and the Sn monomers in toluene solution showed respectable fluorescence quantum yields of 0.60 and 0.18, respectively. Figure 3 displays the normalized absorption and fluorescence spectra for the Ge monomer. The dimers showed no fluorescence signals close to the absorption peaks, but very weak emissions were detected in the near-IR region between ca. 7000 and 12 000 cm^{-1} for the Si−O−Ge and Si−O−Sn dimers. These observations parallel those of Oddos-Marcel et al. for a Si−O−Si dimer.[14]

This lack of fluorescence from $|+\rangle$ confirms the hypothesis that internal conversion between upper and lower exciton states is rapider than the radiative process $|+\rangle \rightarrow S_0$ (vide infra). The pure electronic transition $|-\rangle \rightarrow S_0$ is forbidden in the exciton model.[16] Oddos Marcel et al.[14] have attributed the weak near-IR emissions to radiative transitions between $|-\rangle$ and the minus vibrational level $|0,\nu^-\rangle$ of the ground state. Our observations agree with those of Oddos-Marcel et al. for the Si−O−Si dimer, but the signal-to-noise was not good enough to detect any significant differences of band onset between the Si−O−Ge and Si−O−Sn dimers. Moreover the differences in blue shift of the absorption spectra (Table 1) are less than 250 cm^{-1}. Thus, the overall conclusion of Oddos-Marcel et al.[14] that the exciton splitting is ca. 3800 cm^{-1} for the Si−O−Si dimer probably holds approximately true for the other two variants.

Supranano second Measurements. Figures 4 and 5 show the transient absorption spectral changes recorded over supranano-second time scales, after a 6 ns excitation pulse at 355 nm. Figure 4 shows the transient behavior of the Sn monomer and Figure 5 depicts that of the Si−O−Sn dimer. These two figures demonstrate that the dimer and the monomer transients are very similar with respect of negative absorption (bleaching) at the ground-state absorption Q- and B- band regions, and a positive absorption with a broad maximum near 530 nm. In addition, the dimer spectrum shows an absorption peak to the red side (740 nm) of the ground-state bleaching signal. The decay kinetics of the 530 and 740 nm features were identical (τ = 300 μs), which implies that the two bands belong to the same transient state. In all probability this state has a broad continuous absorption from ca. 400 nm to ca. 780 nm, superimposed upon which is the intense ground-state bleaching signal at 640 nm. The Si−O−Si and Si−O−Ge dimers exhibit a similar behavior to the Si−O−Sn dimer. In all cases the time decay of the 530 nm absorption and the repopulation at the ground-state wavelength were connected by an intervening isosbestic point.

Other p-block metal phthalocyanines studied in this and in other laboratories show transient absorptions in the 500−550 nm region which have been assigned to T_1 to T_n transitions.[29,36−39] Moreover Ferencz et al.[13] have reported a transient absorption spectrum very similar to that shown in Figure 5 for a Si−O−Si dimer and assigned it to the triplet−triplet spectrum of the dimer. The appearance of the isosbestic point between the ground-state bleaching and the positive absorption indicates that the decay of the 530 nm species is responsible for repopulating the ground state without any intermediate entities. Thus, it is reasonable to conclude that the 530 nm transient absorptions observed for the three dimers arise from the T_1 to T_n transitions. The values of the extinction coefficients and quantum yields for the three dimers and the Ge and Sn monomers are collected in Table 2. The table shows that the dimer triplets are not very different from the monomer triplets in both natural lifetime and in quantum yield. This similarity does not extend to interaction with molecular oxygen, as described in the next section.

Oxygen Quenching and Singlet Oxygen Formation. In toluene solutions in the presence of dissolved oxygen, the triplet states of the Ge and Si monomers decayed exponentially to a zero baseline. The rate constant of the decay was directly proportional to [O_2] whence the bimolecular rate constant was extracted. The values (Table 2) of near 2×10^9 M^{-1} s^{-1} are as anticipated for oxygen quenching of a triplet state having an energy level higher than that of $O_2(^1\Delta_g)$ such that the reaction proceeds down the energy gradient. Table 1 also shows that Φ_Δ values were close to the Φ_T values, as is typical for metal phthalocyanines of the p-block metals.

The situation changes dramatically for the dimer species. Figure 6 shows a time profile obtained in air-saturated toluene containing 5 μM Si−O−Sn dimer. The decay is not exponential but could be fitted by a sum of two exponentials; the rate

constant of the fast component was found to be first order in both $[O_2]$ and [Pc], and the slower component was independent of these parameters. In addition the amplitude ratio of the fast-to-slow components, extrapolated to $t = 0$, depended on the solute concentrations. Parallel behavior was noted for the other two dimers. This behavior is typical of a reversible energy transfer reaction involving ^{3}Pc* and O_2. Such reversibility has been observed with several metal phthalocyanines and derivative species having triplet states with energies close to, or slightly below, that of singlet oxygen.[32,39,40] However, there is an additional factor here that must be taken into account, and this is that the singlet oxygen quantum yields for the dimers are very much lower than the quantum yields of the triplet states (Table 2). This is not the case for the monomeric compounds studied earlier.

The kinetic situation can be summarized in the reaction scheme:

$$^3\text{Pc}^* + \text{O}_2(^3\textstyle\sum_g^-) \underset{k_{rev}}{\overset{k_{for}}{\rightleftharpoons}} \text{Pc} + \text{O}_2(^1\Delta_g)$$

$$^3\text{Pc}^* + \text{O}_2(^3\textstyle\sum_g^-) \xrightarrow{k_q} \text{Pc} + \text{O}_2(^3\textstyle\sum_g^-)$$

where k_{for} and k_{rev} are the bimolecular rate constants of the forward and reverse reactions that sustain the equilibrium and k_q is the bimolecular rate constant of the oxygen-induced intersystem crossing process in which the reactants reach the ground-state surface, thereby reducing the quantum yield of singlet oxygen.

In this scheme, the fast decay component in Figure 6 represents the approach to the equilibrium state and the slower component arises from the decay of the equilibrium state due to the fact that both triplet phthalocyanine and singlet oxygen are transient species.[39] When the approach to the equilibrium state is significantly more rapid than the equilibrium state decay (as here), it can be shown that the rate constant of the fast contributor (k_{fast}) is described by

$$k_{fast} = \{k_{for} + k_q\}[O_2] + k_{rev}[\text{Pc}]$$

Thus, the observed rate constant is expected to be first order in both solute concentrations. The inset to Figure 6 shows such a plot for the Si−O−Sn dimer, which is typical of the three dimers studied. Values of k_{rev} were extracted from the slopes of plots such as that shown in Figure 6 (inset) and values of k_{for} and k_d were obtained from the intercepts, slopes, and the quantum yield data as follows.

Defining $S_\Delta = k_{for}/k_{for} + k_d = \Phi_\Delta/\Phi_T$ and with intercept $= \{k_{for} + k_d\}[O_2]$ and Slope $= k_{rev}$ then intercept $= k_{for}[O_2]]/S_\Delta$, and $k_{for} = \text{Intercept}(S_\Delta/[O_2])$, and $k_d = \text{Intercept}/[O_2] - k_{for}$, the values of k_{for} and k_{rev} lead to values for the equilibrium constant K_{eq} $(= k_{for}/k_{rev})$ for the reversible energy transfer reaction. The collected data are listed in Table 2. In addition the preexponential components of the fast and slow components of the decay profiles are proportional to the concentrations of initial T_1 state formed by the laser pulse and to the equilibrium ratio, respectively. These were evaluated from the decay profiles such as that in Figure 6. These results lead to an evaluation of K_{eq}. Both methods yield comparable values for $K_{eq.}$ On the reasonable assumption that converting from ground to excited-state surfaces is devoid of any entropy requirements, the $\Delta G°$ values represent the enthalpy differences between the dimer triplet states and singlet oxygen ($E_\Delta = 22.5$ kcal mol^{-1}). This leads directly to values for the dimer triplet energies that are listed in Table 2.[41] All three dimer triplet states are lower lying than the $^1\Delta_g$ state of oxygen. The order of the triplet energies is Si < Ge < Sn which reflects the magnitude of the spectral shifts in the ground-state absorption spectra and the increase in the inter-ring spacing.

The blue shifts in the ground-state spectra upon dimerization are due to exciton interactions in the cofacial dimers. Triplet state dimers are not subject to exciton behavior because the transition dipole moments for S to T transitions are vanishingly small.[16] However charge resonance interactions are possible in which the excitation is regarded as being delocalized over both monomer units in the dimer.[42] If this is the case here, then these interactions will lead to significant energy lowering in the triplet manifold. For example, the triplet energy of typical monomeric main group metal phthalocyanines such as ZnPc and MgPc are close[43] to 26 kcal mol^{-1}, and thus significantly above the singlet oxygen energy (22.5 kcal mol^{-1}). Here (Table 2) it is shown that Si−O−Si dimer triplet is ca. 7 kcal mol^{-1} or ca. 2500 cm^{-1} lower than this, with the other dimers having triplet states only a little higher.

These conclusions are at variance with those of Ferencz et al. who studied a variant of the Si−O−Si dimer investigated here.[13] With a combination of laser-induced opto-acoustic measurements and some reasonable assumptions, they concluded that the dimer triplet energy was close to that of the monomer triplet viz. in the region of 26.2 kcal mol^{-1}. The oxygen quenching studies conducted here demonstrate conclusively that the energy transfer from dimer triplets to molecular oxygen is indeed an endoergic process, requiring that the triplet energy be lower than 22.5 kcal mol^{-1}.

Ultrafast Pump−Probe Measurements. Figure 7 depicts the time-resolved spectra obtained after absorbing a short (100 fs) laser pulse at 640 nm into a ca. 10 μM solution of the Si−O−Sn dimer in toluene. The spectral features at the first recorded delay time (10 ps) are a positive absorption band with a broad maximum near 580 nm and a bleaching of the ground-state absorption at 643 nm. As time proceeds up to ca. 300 ps post-pulse, the 580 nm absorption undergoes decay to a nonzero level; this residual absorption has a maximum near to 510 nm (Figure 7, inset), a shoulder to the red side, and undergoes no further decay on the subnanosecond time scale. Concomitant with this decay is a filling in at the ground-state wavelength (643 nm) and an isosbestic point near 615 nm (Figure 7) connects these two kinetic features. The spectrum at 300 ps (Figure 7, inset) is very reminiscent of that generated immediately in the supra-nanosecond experiment (Figure 5) and assigned to the dimer triplet state.

The subnanosecond ground-state repopulation time profile could be fitted by a mono exponential approaching a nonzero baseline (Figure 8). The exponential segment had a lifetime that depends on the metal center, viz., 128 ps for the Si−O−Si dimer, 197 ps for the Si−O−Ge dimer, and 103 ps for the Si−O−Sn dimer. The promptly formed absorption at 580 nm is assigned to the lower exciton state of the μ-oxo dimers, generated by a rapid internal conversion process from the upper exciton state. It is unlikely to be due to the upper exciton state itself since a lifetime of >100 ps for the upper exciton state would be large enough that significant fluorescence from that state would be observed. Furthermore, the blue shifts in the ground-state spectra of the dimers with respect to the Si monomer indicate that the energy difference between the upper and lower exciton states is near 1800 cm^{-1}. Such a low energy gap would imply that internal conversion from the upper state would be much more rapid. These considerations lead to the conclusion that the decay of the 580 nm species (and the

concomitant ground-state recovery component) are due to intersystem crossing from the lower singlet exciton state to the triplet manifold. Such a process generates a triplet state that exhibits an absorption maximum at 540 nm and shows no decay on the time scale of Figure 8 (vide supra). The triplet quantum yield of the Si−O−Sn dimer was determined to be 0.35, which implies that 65% of the primarily excited states decay directly through internal conversion to the ground-state surface. This explains why the S_1 to T_1 conversion is accompanied by partial recovery of ground-state absorption (at 643 nm). No such recovery would be observed if the intersystem crossing efficiency would be one. The S−O−Si and Si−O−Ge dimers show similar behavior when compared to the Si−O−Sn dimer. The major difference is that the lifetimes of the lower exciton singlet states and the intersystem crossing yields vary within the series. These data allow the calculation of the rate constants for intersystem crossing (Table 2). As obvious from that table, the k_{ISC} value is largest for the Si−O−Sn dimer, which is probably due to the high Z value of tin enhancing spin−orbital interactions.

The higher time resolution observations that are depicted in Figures 8 and 9 for the Si−O−Si dimer are intriguing. Spectrum A in Figure 9 is the "negative time" spectrum, i.e., that recorded when the probe pulse reaches the sample ahead of the 640 nm pump pulse. This demonstrates the excellent signal-to-noise and zero balance of the spectrometer. Spectrum B is that recorded immediately after the ca. 300 fs rise time of the spectrometer. This shows broad peaks at 540 and 600 nm. This increases in amplitude over some 45 ps (rise lifetime of ca. 10 ps) to a species having broader, less defined peaks throughout the 540 to 600 nm region (spectrum C). During this same time frame, there was some ground state recovery at 635 nm, but no isosbestic point was detected. Eventually the growth turns to decay and at 760 ps post onset (spectrum D) the spectral features of the triplet state are revealed (as detailed above). Figure 10 presents time profiles of the early post-excitation events.

In the preceding paragraph this >100 ps lifetime decay was attributed to intersystem crossing from the lower exciton state. Hence the growth of this absorption in the first 45 ps might be ascribed to internal conversion from the upper exciton state, in which case the zero time spectrum would be that of $|+\rangle$. Several factors mediate against this assignment, however. One is the lack of an isosbestic point in the spectra prior to 45 ps. If $|+\rangle$ were converting to $|-\rangle$ with a concurrent ground-state repopulation, isosbestic behavior would be expected. Moreover, from the magnitude of the blue shift in the ground-state spectra, the exciton splitting is estimated to be near 3800 cm^{-1}. Such a small energy gap would be expected to result in subpicosecond nonradiative decay lifetimes between states of like multiplicity. Support for this comes from recent ultrafast absorption experiments, which have demonstrated that inter-exciton state relaxation occurs in a few tens of femtoseconds in allophycocyanine trimers[44] and within 500 fs in porphyrin arrays[45] where the exciton splitting is near 3000 cm^{-1}.

A qualitative explanation of the early phase dynamics is hinted at by scrutiny of the ground-state absorption spectra of the dimers, best seen from the inset in Figure 2. In contrast to the Q-band region of the monomer systems which show well-resolved vibrational structure, the dimers show a sharp Q-band superimposed on broad structureless absorptions extending >100 nm to the red side of the major peaks. The spectra of cofacial dimers induced by alkali metal ion coordination of metal phthalocyanines with crown ether peripheral substitution show no such broad absorption features.[46] In such compounds D_{4h} symmetry is upheld by the prevention of staggering torsion by the nature of the binding. In the μ-oxo dimers, dimerization is achieved through the presence of a single covalent Si−O−M linkage, about which torsion occurs. These torsional motions give rise to an ensemble of conformations in which the D_{4h} symmetry is broken, causing the observed significant extinction in the red and blue wings of the 0,0 transition. With this in mind, excitation of the dimers at 640 nm (within the intense 0,0 band) leads to population of $|+\rangle$, largely in D_{4h} symmetry. This is followed very rapidly (within the response function of the instrument) by isothermal crossing to an upper torsional/vibrational state of the lower exciton state, which loses its excess energy with a 10 ps relaxation time to generate the thermally equilibrated $|-\rangle$, state. A requirement of this mechanism is that the hot and cold exciton states have the different absorption characteristics observed in Figure 9. The early time changes occur without isosbestic behavior, which supports the assignment of a vibrational cooling process.

Acknowledgment. This work was supported in part by NIH grant CA46281 and by the Center for Photochemical Science at Bowling Green State University. Instrumentation was purchased in part by a grant from the National Science Foundation (CHE 9601516).

References and Notes

(1) Leznoff, C. C., Lever, A. B. P., Eds. *Phthalocyanines: Properties and Applications*; VCH Publishers: New York, 1996; Vols. I−IV.
(2) Joyner, R. D.; Kenney, M. E. *Inorg. Chem.* **1962**, *1*, 236.
(3) Kroenke, W. J.; Sutton, L. E.; Joyner, R. D.; Kenney, M. E. *Inorg. Chem.* **1963**, *2*, 1064.
(4) Esposito, J. N.; Lloyd, J. F.; Kenney, M. E. *Inorg. Chem.* **1966**, *5*, 1979.
(5) Kane, A. R.; Sullivan, J. F.; Kenny, D. H.; Kenney, M. E. *Inorg. Chem.* **1970**, *9*, 1445.
(6) Hush, N. S.; Woolsey, I. S. *Mol. Phys.* **1970**, *21*, 465.
(7) Dirk, C. W.; Inabe, T.; Schoch, K. F., Jr.; Marks, T. J. *J. Am. Chem. Soc.* **1983**, *105*, 1539.
(8) Ciliberto, E.; Doris, K. A.; Pietro, W. J.; Reisner, G. M.; Ellis, D. E.; Fragala, I.; Herbstein, F. H.; Ratner, M. A.; Marks, T. J. *J. Am. Chem. Soc.* **1984**, *106*, 7748.
(9) Anderson, A. B.; Gordon, T. L.; Kenney, M. E. *J. Am. Chem. Soc.* **1985**, *107*, 192.
(10) Sirlin, C.; Bosio, L.; Simon, J. *J. C. S. Chem. Commun.* **1987**, 379.
(11) Orti, E.; Bredas, J. L.; Clarisse, C. *J. Chem. Phys.* **1990**, *92*, 1228.
(12) Ishikawa, N.; Ohno, O.; Kaizu, Y.; Kobayashi, H. *J. Phys. Chem.* **1992**, *96*, 6, 8832.
(13) Ferencz, A.; Neher, D.; Schulze, M.; Wegner, G.; Viaene, L.; De Schryver, F. C. *Chem. Phys. Lett.* **1995**, *245*, 23.
(14) Oddos-Marcel. L.; Madeore, F.; Bock, A.; Neher, D.; Ferencz, A.; Rengel, H.; Wegner, G.; Kryschi, C.; Trommsdorff, H. P. *J. Phys. Chem.* **1996**, *100*, 11850.
(15) Kleinwaechter, J.; Hanack, M. *J. Am. Chem. Soc.* **1997**, *119*, 10684.
(16) Kasha, M. *Radiat. Res.* **1963**, *20*, 55.
(17) Gouterman, M.; Holten, D.; Lieberman, E. *Chem. Phys.* **1977**, *25*, 139.
(18) Sauer, T.; Caseri, W.; Wegner, G.; Vogel, A.; Hoffman, W. *J. Phys. D: Appl. Phys.* **1990**, *23*, 79.
(19) Kaldova, K.; Bank, R.; Ferencz, A.; Neher, D.; Wegner, G. *Mol. Cryst. Liq. Cryst.* **1994**, *252*, 223.
(20) Ern, J.; Bock, A.; Oddos-Marcel. L.; Rengel, H.; Wegner, G.; Trommsdorff, H. P.; Kryschi, C. *J. Phys. Chem. A* **1999**, *103*, 2446.
(21) Wheeler, B. L.; Nagasubramanian, G.; Bard, A. J.; Schechtman, L. A.; Dininny, D. R.; Kenney, M. E. *J. Am. Chem. Soc.* **1984**, *106*, 7404−4710.
(22) Joyner, R. D.; Kenney, M. E. *J. Am. Chem. Soc.* **1960**, *82*, 5790−5791.
(23) Ford, W. E.; Rodgers, M. A. J.; Schechtman, L. A.; Sounik, J. R.; Rihter, B. D.; Kenney, M. E. *Inorg. Chem.* **1992**, *31*, 3371−3377.
(24) Kroenke, W. J.; Kenney, M. E. *Inorg. Chem.* **1964**, *3*, 251−254.
(25) Shutt, J. D.; Batzel, D. A.; Sudiwala, R. V.; Rickert, S. E.; Kenney, M. E. *Langmuir* **1988**, *4*, 1240−1247.
(26) DeWulf, D. W.; Leland, J. K.; Wheeler, B. L.; Bard, A. J.; Batzel, D. A.; Dininny, D. R.; Kenney, M. E. *Inorg. Chem.* **1987**, *26*, 266−270.
(27) Karstens, T.; Kobs, K. *J. Phys. Chem.* **1980**, *74*, 1871.

(28) Wessels, J. M.; Rodgers, M. A. J. *J. Phys. Chem*. **1995**, *99*, 15725.
(29) Rihter, B. D.; Kenney, M. E.; Ford, W. E.; Rodgers, M. A. J. *J. Am. Chem. Soc*. **1990**, *112*, 8064.
(30) Venediktov, V. A.; Krasnovsky, A.A. *Zh. Prokl. Spektrosk*. **1982**, *36*, 152.
(31) Carmichael, I.; Hug, G. L. *J. Phys. Chem. Ref. Data* **1986**, *15*, 1.
(32) Aoudia, M.; Cheng, G.; Kennedy, V. O.; Kenney, M. E.; Rodgers, M. A. J. *J. Am. Chem. Soc.* **1997**, *119*, 6029.
(33) Gorman, A. A.; Hamblett, I.; Rodgers, M. A. J. *J. Am. Chem. Soc*. **1984**, *106*, 4679.
(34) Gorman, A. A.; Hamblett, I.; Lambert, C.; Prescott, A. L.; Rodgers, M. A. J.; Spence, H. M. *J. Am. Chem. Soc.* **1987**, *109*, 3091.
(35) Nikolaitchik, A. V.; Korth, O.; Rodgers, M. A. J. *J. Phys. Chem. A* **1999**, *103*, 7587.
(36) Nikolaitchik, A. V.; Rodgers, M. A. J. *J. Phys. Chem. A* **1999**, *103*, 7597.
(37) Rihter, B. D.; Bohorquez, M. D.; Rodgers, M. A. J.; Kenney, M. E. *Photochem. Photobiol.* **1992**, *55*, 677.
(38) Ford, W. E.; Rihter, B. D.; Kenney, M. E.; Rodgers, M. A. J. *Photochem. Photobiol.* **1989**, *50*, 277.
(39) Firey, P. A.; Ford, W. E.; Sounik, J. R.; Kenney, M. E.; Rodgers, M. A. J. *J. Am. Chem. Soc.* **1988**, *110*, 7626.
(40) Ford, W. E.; Rihter, B. D.; Kenney, M. E.; Rodgers, M. A. J. *J. Am. Chem. Soc.* **1989**, *111*, 2362.
(41) In the forward process in eq 1, only one-ninth of the encounter complexes have singlet multiplicity; for the reverse process all are uniquely singlet. Thus the value of the triplet energy derived from equilibrium studies (as here) will be depressed from the spectroscopic value by a factor of RT ln(1/9). This factor has been accounted for in the values of E_T quoted in Table 2.
(42) Ishii, K.; Yamauchi, S.; Ohba, Y.; Iwaizumi, M.; Uchiyama, I.; Hirota, N.; Maruyama, K.; Osuka, A. *J. Phys. Chem*. **1994**, *98*, 9431.
(43) Darwent, P. D.; Douglas, A.; Harriman, A.; Porter, G.; Richoux, M. C. *Coord. Chem. Rev.* **1982**, *44*, 83.
(44) Edington, M. D.; Riter, R. E.; Beck, W. F. *J. Phys. Chem*. **1996**, *100*, 14206.
(45) Cho, H. S.; Song, N. W.; Kim, Y. H.; Jeoung, S. C.; Hahn, S.; Kim D.; Kim, S. K.; Yoshida, N.; Osuka, A. *J. Phys Chem. A* **2000**, *104*, 3287.
(46) Kobayashi, N.; Lever, A. B. P. *J. Am. Chem. Soc*. **1987**, *109*, 7433.